1    Characterization and Demonstration of value of a Lethal Mouse Model of Middle East

2    Respiratory Syndrome Coronavirus Infection and Disease

3    Xinrong, Tao[1*], Tania Garron[1*], Agrawal, Anurodh Shankar[1*], Abdullah Algaissi[1,8], Bi-Hung

4    Peng[2], Maki Wakamiya[3], Teh-Sheng Chan[1], Lu Lu[4], Lanying Du[5], Shibo Jiang[5], Robert B.

5    Couch[6], and Chien-Te K. Tseng[1,7#]

6

7    Departments of Microbiology and Immunology[1], Pathology[2], Transgenic Mouse Core Facility,

8    Institute for Translational Sciences and Animal Resource Center[3], Internal Medicine, Division of

9    Infectious Disease[6], and Center for Biodefense and Emerging Infectious Disease[7], University of

10   Texas Medical Branch, Galveston, Texas. Institute of Medical Microbiology[4], Fudan University,

11   Shanghai, China, Lindsley F. Kimball Research Institute[5], New York Blood Center, New York,

12   NY. Department of Medical Laboratories Technology[8], College of Applied Medical Sciences,

13   Jazan University, Jazan, KSA.

14   [*] Equal contributors

15   [#] Corresponding author: Department of Microbiology and Immunology, University of Texas

16   Medical Branch, 301 University Boulevard, Galveston National Laboratory 5.200Q, Galveston,

17   TX 77555-0609, Phone: (409)266-6929; FAX: (409)747-0762; e-mail: sktseng@utmb.edu

18   Running title: Transgenic mice for MERS-CoV infection and disease

19

20   Word counts:

21   Abstract:246                                                    Text:5,573

22

23  **Abstract**

24      Characterized animal models are needed for studying pathogenesis of and evaluating

25  medical countermeasures for the persisting Middle East Respiratory Syndrome-Coronavirus

26  (MERS-CoV) infection. Here, we further characterized a lethal transgenic mouse model of

27  MERS-CoV infection and disease that globally expresses hCD26/DPP4. The 50% infectious

28  dose ($ID_{50}$) and lethal dose ($LD_{50}$) of virus were estimated to be <1 and 10 $TCID_{50}$ of MERS-

29  CoV, respectively. Neutralizing antibody developed in surviving mice from the $ID_{50}/LD_{50}$

30  determinations and all were fully immune to challenge with 100 $LD_{50}$ of MERS-CoV. The tissue

31  distribution and histopathology in mice challenged with a potential working dose of 10 $LD_{50}$ of

32  MERS-CoV was subsequently evaluated.  In contrast to the overwhelming infection in mice

33  challenged with $10^5$ $LD_{50}$ of MERS-CoV, we were only able to infrequently recover infectious

34  virus from these mice although qRTPCR tests indicated early and persistent lung infection and

35  delayed occurrence of brain infection. Persistent inflammatory infiltrates were seen in the lungs

36  and brain stems at day 2 and day 6 after infection, respectively. While focal infiltrates were also

37  noted in the liver, definite pathology was not seen in other tissues. Finally, using a receptor

38  binding domain protein vaccine and a MERS-CoV fusion inhibitor, we demonstrated the value of

39  this model for evaluating vaccines and antivirals against MERS. As outcomes of MERS-CoV

40  infection in patients differ greatly, ranging from asymptomatic to overwhelming disease and

41  death, having available both an infection and a lethal model makes this transgenic mouse model

42  relevant for advancing MERS research.

43

44

45 **Importance**

46     Fully characterized animal models are essential for studying pathogenesis and for

47 preclinical screening of vaccines and drugs against MERS-CoV infection and disease. When

48 given a high-dose of MERS-CoV, our transgenic mice expressing hCD26/DPP4 viral receptor

49 uniformly succumbed to death within 6 days, making it difficult to evaluate host responses to

50 infection and disease. We further characterized this model by determining both the $ID_{50}$ and

51 $LD_{50}$ doses of MERS-CoV in order to establish both an infection and a lethal model for MERS

52 and followed this by investigating antibody responses and immunity of mice survived from

53 MERS-CoV infection. Using the estimated $LD_{50}$ and $ID_{50}$ doses, we dissected the kinetics of

54 viral tissue distribution and pathology in mice challenged with 10 $LD_{50}$ of virus, and utilized the

55 model for preclinical evaluation of a vaccine and drug for MERS-CoV infection. This further

56 characterized transgenic mouse model will be useful for advancing MERS research.

57

58

**Introduction**

Severe acute respiratory syndrome (SARS)-coronavirus (CoV) emerged in Asia in 2002 and spread within months to other countries worldwide, including the United States and Canada, resulting in more than 8,000 cases of severe respiratory illness worldwide with a cases-mortality rate of ~10% before being brought under control using infection control measures (1). Ten years later (2012), another new CoV emerged in the Middle East as a cause of severe respiratory disease in humans, and was named Middle East Respiratory Syndrome (MERS)-CoV (2, 3). Unlike the apparently high human-to-human transmissibility but short-lived SARS epidemic, MERS has continued to occur, especially in the Kingdom of Saudi Arabia, and recently appeared in the Republic of South Korea despite an apparent lower inter-human transmission rate than for SARS (4). As of July 3, 2015, more than 1,365 laboratory-confirmed cases of MERS-CoV disease, including at least 487 related deaths, have been identified globally (http://www.who.int/csr/don/03-july-2015-mers-korea/en/). No vaccines or antivirals known to be effective for control of MERS-CoV infection and disease in humans are currently available.

Animal models are needed for study of MERS CoV infection and disease. Nonhuman primates (NHPs), such as rhesus macaques and marmosets, are naturally permissive to MERS-CoV infection and disease (5, 6) but they are expensive models of limited availability. Optimal development of knowledge and preventives and treatments for a new infectious disease of humans requires a small animal model to provide the numbers of animals needed for controlled and extensive studies of pathogenesis and immunity as well as for development of vaccines and antivirals. Mice are the most desirable small animal for this purpose because of availability and existence of a thorough knowledge base, particularly of genetics and immunology. Unfortunately, the standard small animals, mice, hamsters and ferrets, all lack the functional

82   MERS-CoV receptor [human (h) CD26/DPP4] and are not susceptible to infection (7-9). Three

83   humanized transgenic mouse models, each with strengths and weaknesses, have been reported,

84   aiming to overcome the deficiency of small animal models that has impaired many aspects of

85   MERS research (10-12). Of the three mouse models that have been described thus far, two are

86   primarily lung infection models that develop a varying extent of lung pathology in response to

87   $10^5$ to $10^6$ 50% tissue culture infectious doses ($TCID_{50}$) of MERS-CoV but lack morbidity (e.g.,

88   weight loss) and mortality; whereas, a transgenic mouse model globally expressing

89   hCD26/DPP4, that was developed in our laboratory, exhibits an acute illness with profound

90   weight loss ($\geq$ 20%), ruffled fur, hunching, squinting, decreased responsiveness to external

91   stimuli, other clinical manifestations, and death within days after given an intranasal (i.n.) dose

92   of $10^6$ $TCID_{50}$ of MERS-CoV.

93   Although these globally expressing hCD26/DPP4 transgenic mice are highly permissive to

94   MERS-CoV infection and disease, the acute onset of severe morbidity and mortality make it

95   difficult to fully investigate the pathogenesis, host immune responses and immunity of the

96   MERS-CoV infection and disease. To further develop this transgenic mouse model for MERS,

97   we determined the 50% lethal dose ($LD_{50}$) and 50% infectious dose ($ID_{50}$) of MERS-CoV and

98   described the  tissue distribution of viral infection and histopathology in the hCD26/DPP4

99   transgene-positive ($Tg^+$) mice challenged with a much lower, potential working dose of MERS-

100  CoV. Finally, we show that these transgenic mice can be used as a robust preclinical model for

101  evaluating the efficacy of vaccines and antivirals against MERS.

102

103  **Material and Methods**

104   **Mice, virus, and cells.** Transgenic mice expressing hCD26/DPP4 were generated in-house in the

105   barrier facility at the University of Texas Medical Branch as previously described (10). All

106   animal studies were conducted strictly following an approved animal protocol and the guidelines

107   and regulations of the National Institutes of Health and AAALAC. The EMC-2012 strain of

108   MERS-CoV, provided by Heinz Feldmann (NIH, Hamilton, MT) and Ron A. Fouchier (Erasmus

109   Medical Center, Rotterdam, Netherlands), was used throughout the study. Briefly, the MERS-

110   CoV-EMC/2012 strain that we received was designated passage zero (P0) and further expanded

111   with three passages in Vero E6 cells (American Type Culture Collection) for generating cell-free

112   P1, P2, and P3 stocks; P3 was used as the working stock for experiments described in this study.

113   The titers of individual stocks, determined by using Vero E6-based infectivity assays, were

114   expressed as 50% tissue culture infectious doses ($TCID_{50}$)/ml. Aliquots of virus stock with an

115   average of $10^7$ TCID50/ml were stored at -80°C.

116

117   **Viral infections.** All of the *in vitro* and animal studies involving infectious MERS-CoV were

118   conducted within approved bio-safety level 3 (BSL-3) and animal BSL-3 laboratories at the

119   National Galveston Laboratory, strictly following approved notification of usage (NOU), animal

120   protocols, and  the guidelines and regulations of the National Institutes of Health and AAALAC.

121   All of the designs and strategies involving intranasal challenge of $Tg^+$ mice with live MERS-

122   CoV were described in individual experiments.

123

124   **Virus isolations**. Collected tissue specimens of lungs, brain, heart, liver, kidney, spleen, and

125   intestine, were weighed and homogenized in phosphate-buffered saline (PBS) containing 10%

126   fetal calf serum (FCS) with a TissueLyser (Qiagen, Retsch, Haan, Germany), as described earlier

127    (10). After clarification of the cellular and tissue debris by centrifugation, the resulting

128    suspensions of infected tissues were titered in the standard Vero E6 cell-based infectivity assays

129    for quantifying yields of infectious virus. The virus titers of individual samples were expressed

130    as $\log_{10}$ TCID$_{50}$ per gram (g) of tissue.

131

132    **RNA extraction and real time RT-PCR.** Tissues collected at indicated times were placed in

133    individual vials containing RNA later solution (Qiagen), weighed, and stored at 4 $^{\circ}$C until used

134    for extracting total RNA. Briefly, tissues were homogenized in 1 ml of TriZol reagent (Life

135    Technologies) with a TissueLyser. After clarifying by centrifugation at 12,000g for 5 min, the

136    resulting suspensions were tested for total RNA, quantification of MERS-CoV-specific RNA that

137    targeted the upstream E (upE) gene and mouse beta (β)-actin gene (internal control), as described

138    previously (10).  Briefly, 0.5 µg of RNA extracted from individual tissues was used in a one-step

139    real-time RT-PCR with a set of primer/probes specific for upE gene of MERS-CoV, using the

140    Superscript III One-step RT-PCR kit (Invitrogen) according to the manufacturer's instructions.

141    The primers and probes used for upE gene of MERS-CoV were as follows: forward, 5'GCC

142    TCTACACGGGACCCATA-3'; reverse, 5'GCAACG CGC GAT TCA GTT-3'; and

143    fluorescence probe, 5-/56-FAM/CTC TTC ACA TAA TCG CCC CGA GCT CG/36-TAMSp/-3.

144    The relative amount of targeted mRNA was obtained by normalizing with endogenous control

145    gene (β-Actin) and expressed as fold change by the standard threshold cycle (ΔΔCT) method.

146

147    **Serological assays.** MERS-CoV-specific neutralizing antibody and S1 protein-specific IgG

148    antibody responses were quantified by a classical infection reduction assay and a standard

149    ELISA, respectively, as described previously (13, 14). For determining neutralizing antibody

150    titers, the standard Vero E6 cell-based micro-neutralization assay was used. Briefly, starting at

151    dilutions of 1:10, 60 μl of serial 2-fold dilutions of heat-inactivated serum specimens obtained

152    from surviving $Tg^+$ mice at 21 dpi via retro-orbital bleeding were transferred into duplicate wells

153    of 96-well plates containing 120 $TCID_{50}$ of MERS-CoV in 60 μl of M-2 medium/per well,

154    giving a final volume of 120 μl/well. The antibody-virus mixtures were incubated at room

155    temperature for one hour before transferring 100 μl of the mixtures (containing 100 $TCID_{50}$ of

156    MERS-CoV) into confluent Vero E6 cell monolayers in 96-well plates. Six wells of Vero E6

157    cells cultured with equal volumes of M-2 medium with or without virus were included in these

158    assays as positive and negative controls, respectively. When the wells of Vero E6 cells infected

159    with virus alone developed advanced cytopathic effects (CPE), the neutralizing capacity of

160    individual serum specimens was determined, based on the presence or absence of CPE.

161    Reciprocals of the last dilutions of serum specimens capable of completely preventing the

162    formation of CPE were used as the neutralizing antibody titer and expressed as neutralizing titer-

163    100% ($NT_{100}$).

164        For quantifying the total MERS-CoV S1-specific IgG antibodies, 96-well ELISA plates

165    were pre-coated with recombinant S1-His protein (1 μg/ml), as described previously (15, 16).

166    After blocking with Tris-buffered saline (TBS) containing 10% FBS and 0.05% Tween 20 (TBS)

167    for 1 hr at room temperature, 50 μl of serial 10-fold dilutions of mouse serum specimens, starting

168    at dilutions of 1:100, were added to the plates (Corning, Cat. No. 3690), incubated for 1 hr at

169    37°C, and thoroughly washed with TBS before adding horseradish peroxidase (HRP)-conjugated

170    anti-mouse IgG (1:4,000) (Southern Biotech, Cat. No.1030-05) for 1 hr at 37°C. For quantifying

171    total specific IgG antibodies, the thoroughly washed plates were incubated in the dark with o-

172    Phenylenediamine dihydrochloride (Sigma, Cat. No. P9187) for 15 min, the reactions were

173    stopped with 1N $H_2SO_4$, and evaluated in an ELISA plate reader (Molecular Device) for

174    measuring the optical density (OD) at 450 nm. The highest dilutions of serum specimens with

175    MERS-CoV S1-specific antibody with a mean OD reading greater than or equal to  2 standard

176    deviation (SD) greater than the mean for specimens of naïve mice were used to define  titers.

177

178    **Histopathology and IHC staining.** Tissue specimens harvested from animals at indicated times

179    after infection were fixed in 10% buffered-formalin for 72 h, transferred to 70% ethanol, and

180    paraffin-embedded for subsequent sectioning and processing for routine hematoxylin-eosin

181    (H&E) staining for assessing pathological changes, as described previously (10). For testing for

182    viral antigens in tissues of infected mice, the standard alkaline phosphatase-based colorimetric

183    indirect IHC staining using a combination of a rabbit anti-MERS-CoV polyclonal antibody,

184    provided by Dr. Heinz Feldmann, NIAID/NIH through Dr. Thomas Ksiazek at UTMB, and a

185    biotinylated swine anti-rabbit immunoglobulin (Dako, Cat. No. E0353) were employed as we

186    previously described (10, 17). Irrelevant rabbit antibodies were also included in this IHC staining

187    as negative controls. Nuclei were counterstained with Mayer's hematoxylin (Fisher Scientific)

188    before subjecting to microscopic examination.

189

190    **Vaccine and Antiviral Evaluations.** Groups of age-matched Tg[+] mice were immunized

191    intramuscularly (i.m.) twice, three-weeks apart, with S377-588-Fc (10 μg in 50 μl of PBS)

192    formulated with an equal amount of MF59 adjuvant (AddaVax[TM], Cat. No. vac-adx-10,

193    InvivoGen) or MF59 alone, designated S377-588-Fc/MF59 and PBS/MF59, respectively. Sera of

194    immunized mice post second immunization were subjected to serological assays for quantifying

195    neutralizing and MERS-CoV S1 protein-specific IgG antibodies.   Immunized mice were

JVI

196    subsequently challenged (i.n.) at day 10 post second immunization with $10^3$ TCID$_{50}$ of MERS-

197    CoV in a volume of 60 µl. Three mice in each group were sacrificed at 3 dpi for quantifying

198    infectious virus and viral RNA expression, whereas the remaining five in each group were

199    monitored daily for morbidity (weight loss) and mortality.

200        Both the preventive and therapeutic efficacy of a recently proven effective fusion

201    inhibitor peptide, HR2M6 (18), were evaluated.  For measuring the prophylactic potential,

202    groups of Tg$^+$ mice were treated (i.n.) with 200 µg of HR2M6 in 50 µl of PBS/per mouse or PBS

203    alone at 1 and/or 4 hrs prior to challenge (i.n.) with 100 TCID$_{50}$ of MERS-CoV in 60 µl. For

204    assessing the therapeutic effect, groups of Tg$^+$ mice previously infected (i.n.) with 100 TCID$_{50}$ of

205    MERS-CoV were treated with 50 µl of PBS or 200 µg of HR2M6 in 50 µl PBS at 1, 12, and 24

206    hrs after infection and then once daily to day 7 p.i. Three mice in each group were sacrificed at 2

207    dpi for assessing yields of infectious virus or viral RNA in lungs, whereas the remaining five

208    animals in each group were monitored daily for morbidity and mortality.

209

210    Statistical Analysis

211    Neutralizing antibody titers and virus titers were averaged for each group of mice. Comparisons

212    were conducted using Students *t* test and 1-way analysis of variance as indicated.

213

214    **Results**

215    *Determination of LD$_{50}$ and ID$_{50}$, immune responses, and immunity of hCD26/DPP4 transgenic*

216    *mice to MERS-CoV infection.*

217        To determine the LD$_{50}$ and ID$_{50}$, we initially administered (i.n.)  serial 10-fold decreasing

218    doses of MERS-CoV from $10^6$ to $10^1$ TCID$_{50}$ in a volume of 60 µl , to groups of four or eight

219    naïve $Tg^+$ mice and monitored them daily for clinical manifestations (weight loss) and mortality

220    for at least 21 dpi. We found that all mice receiving virus dosages of $10^2$ to $10^6$ $TCID_{50}$ of

221    MERS-CoV succumbed to the infection (100% mortality) with day of death later with reducing

222    dosage (Table 1). Weight loss was extreme ($\geq$20%) for dosages of $10^3$ and higher; all mice given

223    a dose of $10^2$ died but weight loss was 8% or less (data not shown). Only 5 of 8 mice given $10^1$

224    died; deaths were between days 8 to 13 p.i. and weight loss was only 4% (Experiment 1, Table

225    1). All of the surviving mice continued to appear well up to 21 dpi when the experiment was

226    terminated.

227          To further assess the $LD_{50}$ and $ID_{50}$ of the MERS-CoV stock, we challenged (i.n.) another

228    four groups of four $Tg^+$ mice with 2-fold decrements of MERS-CoV, starting from 10 $TCID_{50}$;

229    dosages were 10, 5, 2.5 and 1.25 $TCID_{50}$ of virus. Mice were followed daily for morbidity

230    (weight loss) and mortality for at least 3 weeks. Although none of the infected mice exhibited

231    any significant weight loss (data not shown), we noted a death at days 9 and 10 in mice infected

232    with 10 $TCID_{50}$ and a single death in mice infected with 5 or 1.25 $TCID_{50}$; whereas, all mice

233    challenged with 2.5 $TCID_{50}$ of MERS-CoV survived without clinical illness (Table 1,

234    Experiment 2). From the data in Table 1, we estimated the $LD_{50}$ and $ID_{50}$ of MERS-CoV for this

235    transgenic mouse model to be 10 and <1 $TCID_{50}$, respectively, further emphasizing the extreme

236    susceptibility of hCD25/DPP4 transgenic mice to MERS-CoV infection and disease.

237          All but one mouse that survived challenge with the low-doses of virus had developed

238    serum neutralizing antibodies and MERS-CoV S1 protein-specific IgG antibodies by 21 days

239    following infection, with $NT_{100}$ and ELISA titers of 1:10 to 1:20 and 1:400 to 1:800, respectively

240    (Table 2). We subsequently challenged (i.n.) these low-dose challenge survivors, along with two

241    naïve $Tg^+$ mice, with $10^3$ $TCID_{50}$ (100 $LD_{50}$) of MERS-CoV at 35 dpi to determine if they had

242   developed immunity to a lethal infection dose. While both naive mice simultaneously challenged

243   lost more than 20% body weight and succumbed to infection within 10 dpi, all mice that had

244   survived the prior low dose challenge, including the one that failed to exhibit a serum antibody

245   response, were immune to a subsequent lethal challenge, surviving without  significant weight

246   loss for more than 3 weeks after re-challenge. The rechallenged mouse without serum antibody

247   in the standardized tests did exhibit evidence of neutralizing and ELISA antibody for lower end

248   point criteria. Thus, these results indicate that previous infection with a non-lethal dose of

249   MERS-CoV was sufficient to induce immune responses that fully protect $Tg^+$ mice against lethal

250   infection.

251

252   *Kinetics and tissue distribution of viral infection in hCD26/DPP4 $Tg^+$ mice challenged with 10*

253   *$LD_{50}$ of MERS-CoV*

254        We have shown that $Tg^+$ mice challenged (i.n.) with $10^6$ $TCID_{50}$ of MERS-CoV suffered

255   profound weight loss of $\geq 20\%$ with 100% death within 6 days after infection. While infectious

256   virus could be readily recovered from the lungs and brains and development of a progressive

257   pneumonia, as evidenced by extensive infiltration of inflammatory cells, was seen, no

258   histopathological lesion was identified in brains of infected mice (10). For determining the tissue

259   distribution of viral infection and histopathology over time with a potential working dose of

260   virus, eighteen age-matched (10-14 weeks old) $Tg^+$ mice were challenged (i.n.) with $10^2$ $TCID_{50}$

261   (10 $LD_{50}$) of  MERS-CoV.  The initial plan was to sacrifice three mice at 2, 4, 6, 8, 10 and 12 dpi

262   for assessing  viral infection in the lungs, brain, heart, liver, kidney, spleen, and intestine by

263   quantifying infectious virus and viral RNA expression using Vero E6 cell-based infectivity and

264  qRT-PCR assays, respectively. Standard immunohistochemistry (IHC) with a rabbit anti-MERS-

265  CoV hyperimmune serum was also performed for detecting viral antigens in tissues.

266      In contrast to the acute onset of extensive weight loss and mortality seen in $Tg^+$ mice

267  infected with a high-dose of MERS-CoV, those challenged with a dose of 10 $LD_{50}$ ($10^2$ $TCID_{50}$)

268  only exhibited a maximum of 8% weight loss before dying. We were able to collect tissues from

269  all three animals at two day intervals up to 8 dpi but from only a single mouse at day 10 and

270  none at day 12 p.i. due to infection-associated deaths. Unlike the consistent recovery of $\geq 10^7$

271  $TCID_{50}$/g of infectious virus from the lungs of mice inoculated with $10^5$ $LD_{50}$ ($10^6$ $TCID_{50}$), we

272  detected a much lower titer of virus from the lung ($\sim 10^{4.6}$ $TCID_{50}$/g) of only a single mouse at

273  days 2 and 4 p.i. (Figure 1A).  Also, we only detected approximately $10^{4.2}$ $TCID_{50}$/g of infectious

274  virus from the brain of a single mouse at 8 dpi (Figure 1B). Additionally, IHC staining with

275  specific rabbit antibodies failed to reveal the expression of viral antigens in paraffin-embedded

276  lung and brain tissues, including those positive for infectious virus (data not shown). All tests for

277  infectious virus from other tissues over time, including liver, spleen, kidneys, and intestines,

278  were negative (data not shown).

279      Although infectious virus could only be sporadically detected, results of qRT-PCR

280  analyses targeting the upstream E gene of MERS-CoV clearly indicated a consistent expression

281  of viral RNA, especially in lungs and brains (Figure 1C). All lung specimens collected over time

282  were positive for viral RNA, with the highest level detected on day 4 p.i.. In contrast, viral RNA

283  was undetectable in brains until day 6; however, expression increased thereafter, reaching the

284  highest level at day 10 p.i..  Although attempts to isolate virus from the GI tract were

285  unsuccessful, viral RNA expression was detected at day 6 and increased thereafter, reaching  a

286  level equivalent to $10^{3.4}$ $TCID_{50}$/g at day 10 p.i. (Figure 1C), an increasing trend also observed in

287    Tg$^+$ mice challenged earlier with a high-dose of virus (10). Viral RNA was detectable in all other

288    tissues over time but at low levels. Taken together, these results indicate that, despite differences

289    in kinetics and intensities of viral infection, lung, brain and, possibly GI tracts appear to be the

290    major tissues supporting MERS-CoV infection in Tg$^+$ mice.

291

292    *Histopathology of hCD26/DPP4 transgenic mice infected with 10 LD$_{50}$ of MERS-CoV*

293        In contrast to the profound gross lesions solely detected in the lungs of animals

294    challenged with $10^6$ TCID$_{50}$ of MERS-CoV, no gross organ pathology was noted in the lungs,

295    brains, and other organs of animals sacrificed at 2 day intervals for virological and histological

296    evaluations. However, microscopic lesions were noted on different days after infection in lungs,

297    brains, and, to a lesser extent, in livers, but not in other tissues examined, including spleens,

298    kidneys, and small intestines. As shown in Figure 2, lung histopathology of infected mice

299    primarily consisted of mild and multifocal perivascular, peribronchial, and interstitial

300    infiltrations with mononuclear cells on days 2 and 4 post-infection (p.i.). The intensity of these

301    pulmonary infiltrates was slightly increased in 2 of 3 animals and moderately increased in one

302    animal at day 6, and reached the maximum in all three animals sacrificed at day 8 p.i. A

303    decreasing trend of the pulmonary inflammatory response was seen in the sole survivor at day 10

304    p.i., suggesting some resolution was underway.

305        Unlike the earlier high-dose viral challenge ($10^6$ TCID$_{50}$/mouse) in which an inconsistent

306    mild perivascular effect was the only pathological change seen in infected brains (10), mice

307    infected with $10^2$ TCID$_{50}$/mouse (10 LD$_{50}$) developed progressive inflammatory responses. As

308    shown in Figure 3, no abnormalities could be detected in brain stem tissues on either days 2 or 4

309    p.i. However, pathological changes consisting of perivascular cuffing, microglia activation, and

310   apoptotic bodies that likely represent neuronal death were noted in brain stem tissues from 6 to

311   10 dpi.   While no intracerebral pathology was seen in brain tissues, a mild meningitis was noted

312   in cerebral tissues from 8-10 dpi.

313       Focal mononuclear infiltrations were noted in liver specimens collected on 6-10 dpi, but

314   not 2 and 4 dpi (data not shown); however, we did not detect definite pathology in kidney, small

315   intestine, and spleen specimens. .

316

317   *hCD26/DPP4 transgenic mice as a robust preclinical model for development of vaccines and*

318   *treatment*

319       Having further characterized this transgenic mouse lineage with regard to the $LD_{50}$ and

320   $ID_{50}$ (Tables 1 &2), we explored whether it can be used as a small and economical animal model

321   for development of vaccines and treatments for MERS-CoV infection and disease. Since MERS-

322   CoV receptor binding domain (RBD)-based subunit vaccine (S377-588-Fc) and fusion inhibitor

323   peptide (HR2M6) have been demonstrated to be preventive and therapeutic candidates for MERS

324   (16, 19, 20), we evaluated their efficacy in our transgenic mice against MERS-CoV infection.

325       For evaluating the efficacy of S377-588-Fc as a subunit vaccine, we first determined its

326   immunogenicity in $Tg^+$ mice by measuring serum neutralizing antibody responses. Specifically,

327   two groups of $Tg^+$ mice (eight animals in each group) were immunized (i.m.) twice at a 3-week

328   interval with S377-588-Fc plus MF59 adjuvant (S377-588-Fc/MF59) or PBS/MF59 (as control).

329   Sera of vaccinated mice were collected at day 10 after the second immunization for assessing

330   immunogenicity in neutralizing antibody tests. As shown in Figure 4A-D, consistent with the

331   absence of any detectable neutralizing antibody response (< 1:10), control mice given

332   PBS/MF59 exhibited $10^{4.9}$ $TCID_{50}$/g of MERS-CoV in lung tissues 2 days after challenge i.n.

333     with 100 $LD_{50}$ ($10^3$ $TCID_{50}$) of MERS CoV and profound weight loss ($\geq$20%) with 100%

334     mortality by 8 dpi.  In contrast, those vaccinated with S377-588-Fc/MF59 elicited an average

335     serum neutralizing antibody ($NT_{100}$) titer of ~1:800. Although none of the three vaccinated and

336     challenged mice tested at day 2 p.i. had infectious virus in lung specimens, the remaining five

337     vaccinated and challenged mice exhibited mild weight loss and a single death occurred at 10 dpi;

338     the remaining four animals recovered from the mild morbidity and survived until the experiment

339     was terminated at day 21 p.i. (data not shown).

340        The efficacy of the HR2M6 virus fusion inhibitor was also evaluated in $Tg^+$ mice. We

341     initially tested it as prophylaxis by intranasal administration of a single dose of 200 µg HR2M6

342     or PBS alone at 1 and 4 hrs before challenging with 10 $LD_{50}$ (100 $TCID_{50}$) of MERS-CoV. Titers

343     of infectious virus and viral RNA in lungs of three animals sacrificed at 2 dpi were determined

344     by Vero E6-based infectivity assays and qRT-PCR, respectively. Although no infectious virus

345     could be recovered from challenged mice regardless of whether treated with HR2M6 or not, lung

346     viral RNA titers were significantly reduced from 3.7 of PBS-treated mice to 1.2 and 1.4 $\log_{10}$

347     $TCID_{50}$ eq./g in those pretreated with HR2M6 at 1 and 4 hrs, respectively (Figure 5A).  All of the

348     remaining five and four out of five mice pretreated with HR2M6 at 1 and 4 hrs, respectively,

349     were protected from death, whereas four out of five PBS-treated mice succumbed to the infection

350     (Figure 5B). To evaluate the therapeutic efficacy of HR2M6, $Tg^+$ mice previously infected with

351     10 $LD_{50}$ ($10^2$ $TCID_{50}$) of MERS-CoV were administered (i.n.) either PBS or 200 µg of HR2M6

352     at 1, 12, and 24 hrs, and then daily after infection until 7 dpi. Three mice were sacrificed at 2 dpi

353     for quantifying viral RNA, whereas the remaining five animals were monitored for morbidity

354     and mortality. In contrast to the earlier report, we did not see any therapeutic benefit of HR2M6

355     as neither the viral load tests nor the mortality rate were significantly reduced (Figure 5C-D) (21,

356  22). Results obtained from additional $Tg^+$ mice treated with this fusion inhibitor prior to and/or

357  post exposure to different doses of MERS-CoV consistently indicated that HR2M6 was effective

358  as a prophylactic, but not as a therapeutic agent against MERS-CoV infection and disease in the

359  $Tg^+$ mouse (data not shown).

360  **Discussion**

361      Using a cytomegalovirus promoter in a manner previously successful for developing

362  transgenic mouse models of SARS-CoV infection and disease, we identified candidate MERS-

363  CoV susceptible transgenic mouse lineages (10). One lineage was selected and further evaluated.

364  A $10^6$ $TCID_{50}$ (Vero cell cultures) intranasal dose of MERS-CoV strain EMC/2012 induced a

365  severe pneumonia leading to death in 4 to 6 days. Lung virus was highest on day 2 post

366  challenge and dissemination then ensued to many other organs including the brain (10). Based on

367  RT-PCR assays, virus titer was highest in lung on day 2 and brain on day 4 post challenge. Both

368  extensive gross and microscopic lung pathology developed. Of interest is that lung

369  histopathology was major on day 4 but brain had minor to no pathology despite detection of high

370  titers of virus and viral antigens in neurons and glial cells. The extensive infection and disease

371  with MERS-CoV in this transgenic mouse model was similar to that reported in marmosets

372  challenged with MERS-CoV (6). A concern was that the challenge to our transgenic mice and

373  that given to marmosets might represent an overwhelming dose in very susceptible animals that

374  caused a very severe acute lung infection with dissemination to numerous organs. Although

375  currently available clinical information is inadequate to exclude dissemination of MERS-CoV as

376  a component of MERS-CoV pneumonia in humans, MERS is considered to be a respiratory

377  infection and disease (23, 24).

378        To clarify the role of challenge dosage in our transgenic mouse model and to provide

379        guidance for study of MERS-CoV infection and disease as well as for evaluation of vaccines and

380        antivirals, we proceeded to conduct infectivity assays in the transgenic mice. These studies

381        yielded an estimated $ID_{50}$ of <1 $TCID_{50}$ (Vero cell cultures) and a $LD_{50}$ of 10 $TCID_{50}$ (Table 1).

382        Thus, the initial challenge study with a challenge dose of $10^6$ $TCID_{50}$ represented a challenge

383        with more than 1 million $ID_{50}$ and 100,000 $LD_{50}$ of virus. This might be designated as an

384        "overwhelming" dosage and suggests that this may have also been true for the marmoset study

385        (6).

386        As indicated earlier, two other MERS-CoV mouse infection models with some associated

387        disease have been reported (11, 12). The approaches used to provide the human DPP4 receptor

388        were transduction with an adenovirus type 5 vector (Ad5), gene replacement with a commercial

389        procedure (VelociGene) and our transgenic method. While challenge dosages for the 3 models

390        (including our model) in the published data were similar, results of challenge differed

391        considerably. Most striking is that the Ad5 and VelociGene models induced lung infections with

392        some histopathology but little to no clinical disease and no mortality. In contrast, our transgenic

393        model also induced lung infection at about the same level but with severe gross and microscopic

394        pathology, virus dissemination to other organs, including brain, and severe clinical disease

395        preceding death in 4 to 6 days. Tests for dissemination were apparently not done for the Ad5

396        model and were limited to brain on days 2 and 4 (reported negative) for the VelociGene model.

397        In the present study, using a lower challenge dosage (10 $LD_{50}$), transgenic mice still exhibited

398        dissemination of virus, including to brain, but this was first detected later (day 6 p.i.). Clinical

399        disease occurred but was milder than seen earlier; however, mortality was still 100% although

400        occurring later (days 6 to 12). Mortality was not reported at these later times for the Ad5 model

401    but the VelociGene model was apparently not followed beyond day 4. In summary, all 3 models

402    appear suitable for studies with desired endpoints of lung virus yield and some lung

403    histopathology. The transgenic models add virus dissemination, severe gross lung pathology and

404    histopathology, severe clinical disease and mortality as potential endpoints for study. Whether

405    either of the other 2 models would have exhibited the more substantial endpoints with higher

406    challenge dosages, more extensive testing or longer follow is unknown.

407        On the basis of available data, it seems reasonable to suggest that virus dissemination and

408    infection of other organs may occur during MERS-CoV infections, particularly in those with

409    severe disease. Virus has been detected in blood and urine of a MERS case (25). Moreover, the

410    receptor for MERS-CoV, CD26/DPP4 (9), is ubiquitous in human tissues, and, presumably, in

411    primates and humanized mice; included are demonstrated presence in lung, kidney, GI tract,

412    brain and most (if not all) other organs (26). Given access to the organ, virus infection may occur

413    and yield virus and local abnormalities.

414        Initial reports of SARS emphasized the lung disease, its severity, and problems in

415    management (1, 27-29). Gastrointestinal infection and disease were reported commonly in early

416    reports as for MERS, but disease in other organs was not. However, subsequent reports of

417    autopsies on SARS related deaths noted dissemination and a high frequency of CNS disease,

418    particularly of neurons (28, 30, 31). It seems possible that an encephalopathy/encephalitis-type

419    of abnormality might have been missed in patients with severe lung disease. In this regard, it is

420    of interest that the reports of infection and disease for the mouse-adapted MA-15 strain of

421    SARS-CoV and the ACE receptor transgenic mouse models that were capable of causing severe

422    disease and death in infected mice exhibited SARS-CoV dissemination and presence of virus in

423    the brain (32-34). Thus, SARS-CoV appears to have a capacity for dissemination with infection

424    and disease in other organs, including brain. In a report of three severe cases of CNS disease in

425    association with MERS, the authors suggested CNS disease might be missed among cases of

426    severe disease cared for in intensive care units with use of sedation and sometimes

427    neuromuscular blockade in the care of patients (35). These findings for SARS-CoV and MERS-

428    CoV infections and diseases in humans suggest a need for caution in drawing conclusions about

429    patterns of human infection and disease until a complete set of data are available. Similarly, data

430    on animal model infections suggest conclusions about properties of a model should await a full

431    characterization of the course of infection and disease in the model.

432         Although further refinement of our transgenic mouse model is desirable, a major value of

433    a small animal model of an infection and disease of humans is for preclinical evaluations of

434    infection and vaccine-induced immunity and of antimicrobials for prevention and treatment. For

435    a test of our model, we conducted a pilot study of immunity induced in surviving mice in the

436    $ID_{50}/LD_{50}$ determinations and a preliminary test of a candidate vaccine and antiviral for MERS-

437    CoV. Mice surviving infection had developed serum neutralizing antibody and all were

438    completely immune to challenge with 100 $LD_{50}$ of MERS-CoV (Tables 1&2). Similarly, a

439    receptor binding domain protein vaccine, S377-588-Fc, induced serum neutralizing antibody to

440    MERS-CoV and vaccinated animals were significantly protected to challenge with 100 $LD_{50}$ of

441    virus (Figure 4). Finally, although no benefit was seen with post challenge treatment in our test,

442    we verified a previous report that intranasal administration of a MERS-CoV fusion inhibitor

443    peptide, HR2M6, before virus challenge prevented disease and death from challenge (Figure 5,

444    (18). Thus, the utility of our MERS-CoV model for studies of immunity and for development of

445    vaccines and antivirals has been demonstrated.

446      Although we have not yet developed a model of infection not leading to death, the ID$_{50}$

447 data available for our virus and test system assure an effort would be successful. A variation in

448 severity and pattern of infection and disease in a MERS-CoV model is potentially important as

449 human infection and disease apparently spans a spectrum from infection with little or no disease

450 to overwhelming disease and death (24, 36). Currently available data indicate that our transgenic

451 mouse model can completely span this spectrum of infection and disease. To have available both

452 an infection and a lethal model of MERS-CoV infection is highly desirable.

453

454 **Acknowledgements**

462

463 **References**

464  1.    **Peiris JS, Guan Y, Yuen KY.** 2004. Severe acute respiratory syndrome. Nature
465          medicine **10:**S88-97.
466  2.    **Assiri A, McGeer A, Perl TM, Price CS, Al Rabeeah AA, Cummings DA,
467          Alabdullatif ZN, Assad M, Almulhim A, Makhdoom H, Madani H, Alhakeem R, Al-
468          Tawfiq JA, Cotten M, Watson SJ, Kellam P, Zumla AI, Memish ZA.** 2013. Hospital
469          outbreak of Middle East respiratory syndrome coronavirus. The New England journal of
470          medicine **369:**407-416.
471  3.    **Guery B, Poissy J, el Mansouf L, Sejourne C, Ettahar N, Lemaire X, Vuotto F,
472          Goffard A, Behillil S, Enouf V, Caro V, Mailles A, Che D, Manuguerra JC, Mathieu
473          D, Fontanet A, van der Werf S.** 2013. Clinical features and viral diagnosis of two cases

474     of infection with Middle East Respiratory Syndrome coronavirus: a report of nosocomial
475     transmission. Lancet **381:**2265-2272.

476  4.  Middle East respiratory syndrome coronavirus (MERS-CoV): Summary and Risk
477     Assessment of Current Situation in Korea and China – as of 3 June 2015
478     http://www.who.int/csr/disease/coronavirus_infections/risk-assessment-3june2015/en/.

479  5.  **de Wit E, Rasmussen AL, Falzarano D, Bushmaker T, Feldmann F, Brining DL,**
480     **Fischer ER, Martellaro C, Okumura A, Chang J, Scott D, Benecke AG, Katze MG,**
481     **Feldmann H, Munster VJ.** 2013. Middle East respiratory syndrome coronavirus
482     (MERS-CoV) causes transient lower respiratory tract infection in rhesus macaques.
483     Proceedings of the National Academy of Sciences of the United States of America
484     **110:**16598-16603.

485  6.  **Falzarano D, de Wit E, Feldmann F, Rasmussen AL, Okumura A, Peng X, Thomas**
486     **MJ, van Doremalen N, Haddock E, Nagy L, LaCasse R, Liu T, Zhu J, McLellan JS,**
487     **Scott DP, Katze MG, Feldmann H, Munster VJ.** 2014. Infection with MERS-CoV
488     causes lethal pneumonia in the common marmoset. PLoS pathogens **10:**e1004250.

489  7.  **Coleman CM, Matthews KL, Goicochea L, Frieman MB.** 2014. Wild-type and innate
490     immune-deficient mice are not susceptible to the Middle East respiratory syndrome
491     coronavirus. The Journal of general virology **95:**408-412.

492  8.  **de Wit E, Prescott J, Baseler L, Bushmaker T, Thomas T, Lackemeyer MG,**
493     **Martellaro C, Milne-Price S, Haddock E, Haagmans BL, Feldmann H, Munster VJ.**
494     2013. The Middle East respiratory syndrome coronavirus (MERS-CoV) does not
495     replicate in Syrian hamsters. PLoS one **8:**e69127.

496  9.  **Raj VS, Smits SL, Provacia LB, van den Brand JM, Wiersma L, Ouwendijk WJ,**
497     **Bestebroer TM, Spronken MI, van Amerongen G, Rottier PJ, Fouchier RA, Bosch**
498     **BJ, Osterhaus AD, Haagmans BL.** 2014. Adenosine deaminase acts as a natural
499     antagonist for dipeptidyl peptidase 4-mediated entry of the Middle East respiratory
500     syndrome coronavirus. Journal of virology **88:**1834-1838.

501  10. **Agrawal AS, Garron T, Tao X, Peng BH, Wakamiya M, Chan TS, Couch RB, Tseng**
502     **CT.** 2015. Generation of a transgenic mouse model of Middle East respiratory syndrome
503     coronavirus infection and disease. Journal of virology **89:**3659-3670.

504  11. **Pascal KE, Coleman CM, Mujica AO, Kamat V, Badithe A, Fairhurst J, Hunt C,**
505     **Strein J, Berrebi A, Sisk JM, Matthews KL, Babb R, Chen G, Lai KM, Huang TT,**
506     **Olson W, Yancopoulos GD, Stahl N, Frieman MB, Kyratsous CA.** 2015. Pre- and
507     postexposure efficacy of fully human antibodies against Spike protein in a novel
508     humanized mouse model of MERS-CoV infection. Proceedings of the National Academy
509     of Sciences of the United States of America **112:**8738-8743.

510  12. **Zhao J, Li K, Wohlford-Lenane C, Agnihothram SS, Fett C, Gale MJ, Jr., Baric RS,**
511     **Enjuanes L, Gallagher T, McCray PB, Jr., Perlman S.** 2014. Rapid generation of a
512     mouse model for Middle East respiratory syndrome. Proceedings of the National
513     Academy of Sciences of the United States of America **111:**4970-4975.

514  13. **Du L, Kou Z, Ma C, Tao X, Wang L, Zhao G, Chen Y, Yu F, Tseng CT, Zhou Y,**
515     **Jiang S.** 2013. A truncated receptor-binding domain of MERS-CoV spike protein
516     potently inhibits MERS-CoV infection and induces strong neutralizing antibody
517     responses: implication for developing therapeutics and vaccines. PLoS one **8:**e81587.

518    14.    **Tseng CT, Sbrana E, Iwata-Yoshikawa N, Newman PC, Garron T, Atmar RL,**
519           **Peters CJ, Couch RB.** 2012. Immunization with SARS coronavirus vaccines leads to
520           pulmonary immunopathology on challenge with the SARS virus. PloS one **7:**e35421.
521    15.    **Ma C, Wang L, Tao X, Zhang N, Yang Y, Tseng CT, Li F, Zhou Y, Jiang S, Du L.**
522           2014. Searching for an ideal vaccine candidate among different MERS coronavirus
523           receptor-binding fragments--the importance of immunofocusing in subunit vaccine
524           design. Vaccine **32:**6170-6176.
525    16.    **Zhang N, Channappanavar R, Ma C, Wang L, Tang J, Garron T, Tao X, Tasneem**
526           **S, Lu L, Tseng CT, Zhou Y, Perlman S, Jiang S, Du L.** 2015. Identification of an ideal
527           adjuvant for receptor-binding domain-based subunit vaccines against Middle East
528           respiratory    syndrome    coronavirus.    Cellular    &    molecular    immunology
529           doi:10.1038/cmi.2015.03.
530    17.    **Tao X, Mei F, Agrawal A, Peters CJ, Ksiazek TG, Cheng X, Tseng CT.** 2014.
531           Blocking of exchange proteins directly activated by cAMP leads to reduced replication of
532           Middle East respiratory syndrome coronavirus. Journal of virology **88:**3902-3910.
533    18.    **Channappanavar R, Lu L, Xia S, Du L, Meyerholz DK, Perlman S, Jiang S.** 2015.
534           Protective Effect of Intranasal Regimens Containing Peptidic Middle East Respiratory
535           Syndrome Coronavirus Fusion Inhibitor Against MERS-CoV Infection. The Journal of
536           infectious diseases doi:10.1093/infdis/jiv325.
537    19.    **Tang J, Zhang N, Tao X, Zhao G, Guo Y, Tseng CT, Jiang S, Du L, Zhou Y.** 2015.
538           Optimization of antigen dose for a receptor-binding domain-based subunit vaccine
539           against MERS coronavirus. Human vaccines & immunotherapeutics **11:**1244-1250.
540    20.    **Wang L, Shi W, Joyce MG, Modjarrad K, Zhang Y, Leung K, Lees CR, Zhou T,**
541           **Yassine HM, Kanekiyo M, Yang ZY, Chen X, Becker MM, Freeman M, Vogel L,**
542           **Johnson JC, Olinger G, Todd JP, Bagci U, Solomon J, Mollura DJ, Hensley L,**
543           **Jahrling P, Denison MR, Rao SS, Subbarao K, Kwong PD, Mascola JR, Kong WP,**
544           **Graham BS.** 2015. Evaluation of candidate vaccine approaches for MERS-CoV. Nature
545           communications **6:**7712.
546    21.    **Gao J, Lu G, Qi J, Li Y, Wu Y, Deng Y, Geng H, Li H, Wang Q, Xiao H, Tan W,**
547           **Yan J, Gao GF.** 2013. Structure of the fusion core and inhibition of fusion by a heptad
548           repeat peptide derived from the S protein of Middle East respiratory syndrome
549           coronavirus. Journal of virology **87:**13134-13140.
550    22.    **Lu L, Liu Q, Zhu Y, Chan KH, Qin L, Li Y, Wang Q, Chan JF, Du L, Yu F, Ma C,**
551           **Ye S, Yuen KY, Zhang R, Jiang S.** 2014. Structure-based discovery of Middle East
552           respiratory syndrome coronavirus fusion inhibitor. Nature communications **5:**3067.
553    23.    **Zaki AM, van Boheemen S, Bestebroer TM, Osterhaus AD, Fouchier RA.** 2012.
554           Isolation of a novel coronavirus from a man with pneumonia in Saudi Arabia. The New
555           England journal of medicine **367:**1814-1820.
556    24.    **Zumla A, Hui DS, Perlman S.** 2015. Middle East respiratory syndrome. Lancet
557           doi:10.1016/S0140-6736(15)60454-8.
558    25.    **Drosten C, Seilmaier M, Corman VM, Hartmann W, Scheible G, Sack S, Guggemos**
559           **W, Kallies R, Muth D, Junglen S, Muller MA, Haas W, Guberina H, Rohnisch T,**
560           **Schmid-Wendtner M, Aldabbagh S, Dittmer U, Gold H, Graf P, Bonin F, Rambaut**
561           **A, Wendtner CM.** 2013. Clinical features and virological analysis of a case of Middle
562           East respiratory syndrome coronavirus infection. The Lancet. Infectious diseases **13:**745-
563           751.

26.  **Gorrell MD.** 2005. Dipeptidyl peptidase IV and related enzymes in cell biology and liver disorders. Clin Sci (Lond) **108:**277-292.

27.  **Denison MR.** 2004. Severe acute respiratory syndrome coronavirus pathogenesis, disease and vaccines: an update. The Pediatric infectious disease journal **23:**S207-214.

28.  **Ding Y, He L, Zhang Q, Huang Z, Che X, Hou J, Wang H, Shen H, Qiu L, Li Z, Geng J, Cai J, Han H, Li X, Kang W, Weng D, Liang P, Jiang S.** 2004. Organ distribution of severe acute respiratory syndrome (SARS) associated coronavirus (SARS-CoV) in SARS patients: implications for pathogenesis and virus transmission pathways. The Journal of pathology **203:**622-630.

29.  **Nicholls JM, Poon LL, Lee KC, Ng WF, Lai ST, Leung CY, Chu CM, Hui PK, Mak KL, Lim W, Yan KW, Chan KH, Tsang NC, Guan Y, Yuen KY, Peiris JS.** 2003. Lung pathology of fatal severe acute respiratory syndrome. Lancet **361:**1773-1778.

30.  **Gu J, Gong E, Zhang B, Zheng J, Gao Z, Zhong Y, Zou W, Zhan J, Wang S, Xie Z, Zhuang H, Wu B, Zhong H, Shao H, Fang W, Gao D, Pei F, Li X, He Z, Xu D, Shi X, Anderson VM, Leong AS.** 2005. Multiple organ infection and the pathogenesis of SARS. The Journal of experimental medicine **202:**415-424.

31.  **Xu J, Zhong S, Liu J, Li L, Li Y, Wu X, Li Z, Deng P, Zhang J, Zhong N, Ding Y, Jiang Y.** 2005. Detection of severe acute respiratory syndrome coronavirus in the brain: potential role of the chemokine mig in pathogenesis. Clinical infectious diseases : an official publication of the Infectious Diseases Society of America **41:**1089-1096.

32.  **McCray PB, Jr., Pewe L, Wohlford-Lenane C, Hickey M, Manzel L, Shi L, Netland J, Jia HP, Halabi C, Sigmund CD, Meyerholz DK, Kirby P, Look DC, Perlman S.** 2007. Lethal infection of K18-hACE2 mice infected with severe acute respiratory syndrome coronavirus. Journal of virology **81:**813-821.

33.  **Roberts A, Deming D, Paddock CD, Cheng A, Yount B, Vogel L, Herman BD, Sheahan T, Heise M, Genrich GL, Zaki SR, Baric R, Subbarao K.** 2007. A mouse-adapted SARS-coronavirus causes disease and mortality in BALB/c mice. PLoS pathogens **3:**e5.

34.  **Tseng CT, Huang C, Newman P, Wang N, Narayanan K, Watts DM, Makino S, Packard MM, Zaki SR, Chan TS, Peters CJ.** 2007. Severe acute respiratory syndrome coronavirus infection of mice transgenic for the human Angiotensin-converting enzyme 2 virus receptor. Journal of virology **81:**1162-1173.

35.  **Arabi YM, Harthi A, Hussein J, Bouchama A, Johani S, Hajeer AH, Saeed BT, Wahbi A, Saedy A, AlDabbagh T, Okaili R, Sadat M, Balkhy H.** 2015. Severe neurologic syndrome associated with Middle East respiratory syndrome corona virus (MERS-CoV). Infection doi:10.1007/s15010-015-0720-y.

36.  **Al-Tawfiq JA.** 2013. Middle East Respiratory Syndrome-coronavirus infection: an overview. Journal of infection and public health **6:**319-322.

607 **FIGURE LEGENDS**

608 **Figure 1. Kinetics and tissue distribution of MERS-CoV infection in hCD26/DPP4**

609 **transgenic mice.** Eighteen hCD26/DPP4 transgene-positive (Tg[+]) mice were challenged i.n.

610 with 10 LD50 ($10^2$ TCID$_{50)}$ of MERS-CoV/mouse in 50 µl. Three animals were euthanized at 2

611 day intervals starting from 2 dpi for assessing the magnitudes of viral infection in tissues by

612 Vero E6-based infectivity and qRT-PCR targeting MERS-CoV-specific E gene. (A) Low levels

613 of virus were recovered from infected lung homogenates of a single mouse (out of three) at 2 and

614 4 dpi. Dotted lines represent "Limit of Detection" (B) A barely detectable level of virus was

615 recovered from brain homogenates of one mouse (out of three) at 8 dpi. Dotted lines represent

616 "Limit of Detection" (C) Kinetics of viral loads in various tissue homogenates harvested at

617 indicated dpi, as assessed by RNA levels of upstream E gene-specific viral RNA expression in

618 tissues harvested at indicated times post infection are shown. Data are presented as Mean ±

619 standard error (SE); error bars indicate standard error.

620

621 **Figure 2. Low and high power photomicrographs of lungs of hCD26/DPP4 Tg[+] mice**

622 **challenged with 10 LD$_{50}$ of MERS-CoV.** H&E stained paraffin-embedded sections of lung

623 specimens collected from Tg[+] mice at indicated days after infection were evaluated for pathology

624 as briefly described in Materials and Methods. Multifocal perivascular and peribronchiolar

625 infiltrates predominately comprised of mononuclear cells were detected at 2 and 4 dpi. The

626 inflammatory responses gradually increased and extended to bronchi and alveolar interstitium

627 through 6-8 dpi. Some resolution was noted at 10 dpi (single surviving mouse) but discrete

628 perivasculitis remained detectable.

629

630 **Figure 3. High power photomicrographs of brain stem and cortex of hCD26/DPP4 Tg[+]**

631 **mice challenged with 10 LD$_{50}$ of MERS-CoV.** Brain tissues obtained from the same infected

632 mice described in Figure 2 were processed for assessing histopathology. No pathological lesions

633 were seen at 2 and 4 dpi. However, pathological changes, including perivascular cuffing,

634 apoptotic bodies, and activated microglia, were seen in the brainstem on days 6 to 10 pi. No

635 intracerebral pathology was seen but mononuclear cell collections in cortical meninges were seen

636 on days 8 and 10 p.i.

637

638 **Figure 4. Immunization of hCD26/DDp4 Tg[+] mice with a receptor binding domain (RBD)**

639 **and challenge with 100 LD$_{50}$ of MERS-CoV.** Two groups of Tg[+] mice, eight animals in each

640 group, were immunized (twice, three-weeks apart) with MF59-adjuvanted RBD fragment fused

641 with Fc or MF59/PBS alone. Resulting neutralizing antibody titers were determined prior to viral

642 challenge (A). Lung viral loads of three animals were determined at day 4 after infection with

643 100 LD$_{50}$ ($10^3$ TCID$_{50}$) of MERS-CoV by qRT-PCR targeting the upstream E gene, and were

644 expressed as $\log_{10}$ TCID$_{50}$ equivalents/per gram (B). The remaining five mice in each group were

645 monitored daily for weight loss (C) and survivor rates (D). Error bars indicate standard error. ***

646 *P* < 0.001, Students *t* test between control and test groups.

647

648 **Figure 5. Prophylactic and therapeutic evaluations of the HR2M6 fusion inhibitor against**

649 **MERS-CoV infection and disease in hCD26/DPP4 transgenic mice,** For evaluating the

650 prophylactic efficacy, groups of Tg[+] mice, eight in each group, were given a single dose of either

651 HR2M6 (200 µg in 60 µl) or PBS (control) at 1 or 4 hrs before viral challenge. Mice were

652 challenged i.n. with 10 LD$_{50}$ ($10^2$ TCID$_{50}$) of MERS-CoV in 60 µl. Lung viral loads were

653 determined in three infected mice per group on day 3 p.i.by qRT-PCR targeting the upstream E

654 gene, and expressed as $\log_{10}$ $TCID_{50}$ equivalents/per gram (A). Error bars indicate standard error.

655 Survivor rates of the remaining five animals in each group were assessed daily (B). For assessing

656 the therapeutic efficacy, two groups of $Tg^+$ mice, eight animals/group, were treated i.n. with

657 HR2M6 (200 µg in 60 µl) or PBS at 1, 12, and 24 hrs and then daily for 7 days after infection,

658 Viral challenge was with $10LD_{50}$ ($10^2$ $TCID_{50}$); viral load was assessed on day 2 p.i.(C) and

659 survivor rates for 12 days (D). ** $P < 0.01$, 1-way analysis of variance (ANOVA) compared with

660 control group.

**A**

Lung viral titers (Log$_{10}$TCID$_{50}$/g)

Days after infection

**B**

Brain viral titers (Log$_{10}$TCID$_{50}$/g)

Days after infection

**C**

Viral load (Log$_{10}$TCID$_{50}$ eq./g)

- 2 dpi
- 4 dpi
- 6 dpi
- 8 dpi
- 10 dpi

Lung   Brain   Liver   Spleen   Kidneys   GI

**2 dpi**

**4 dpi**

**6 dpi**

**8 dpi**

**10 dpi**

500μM

100μM
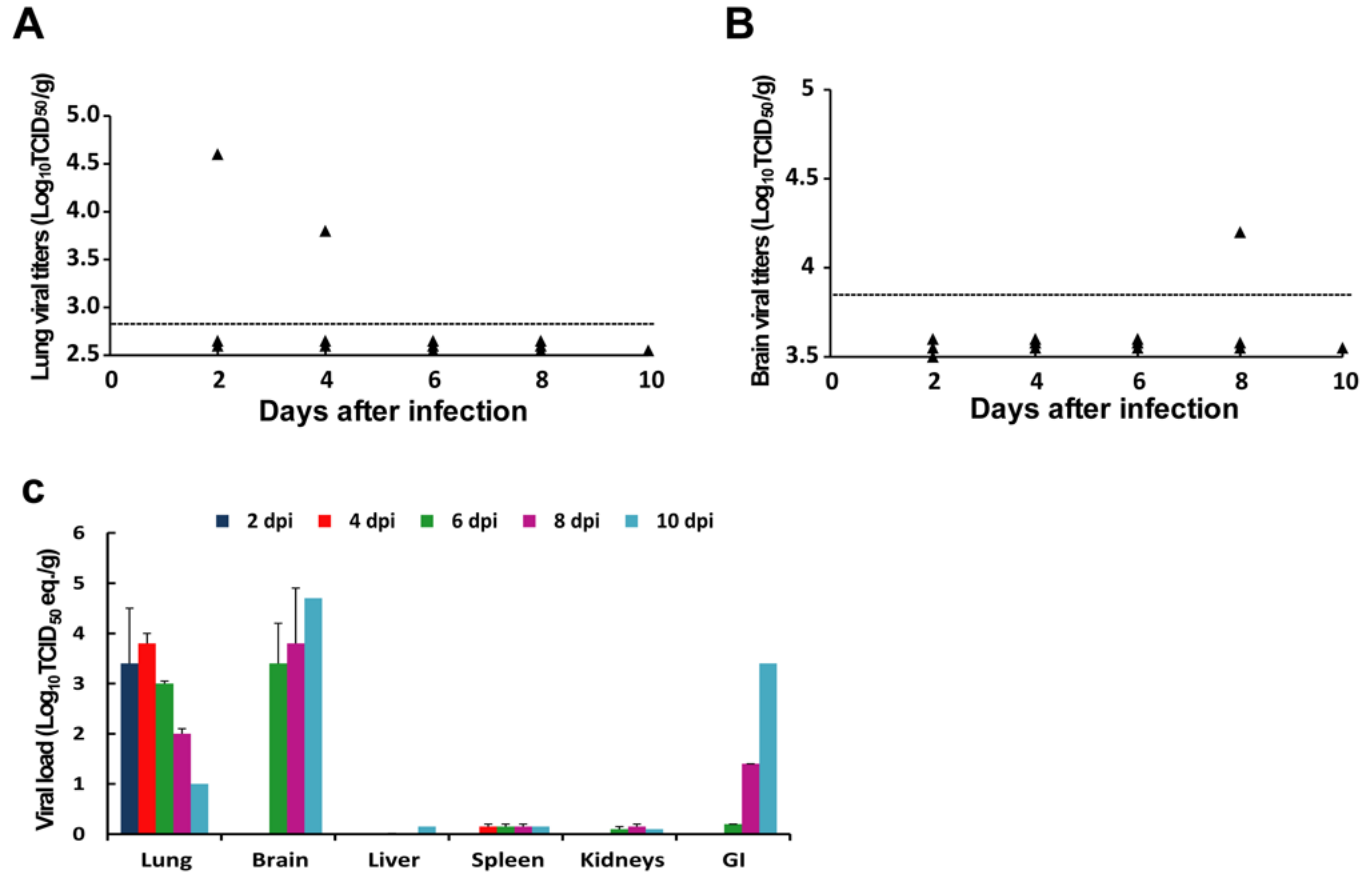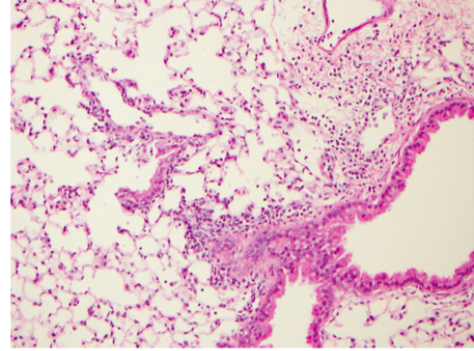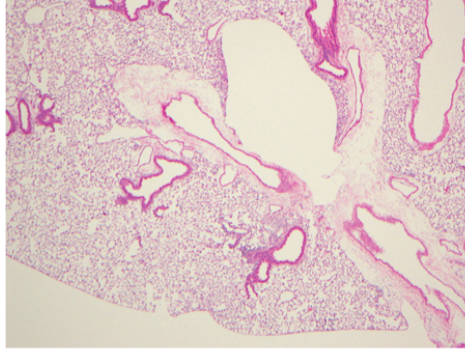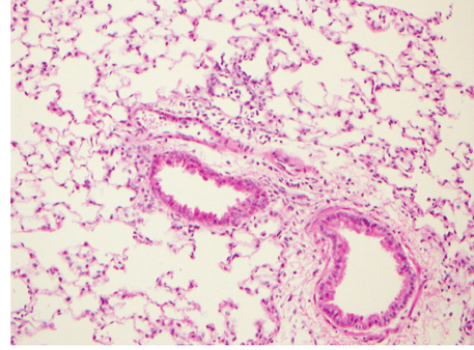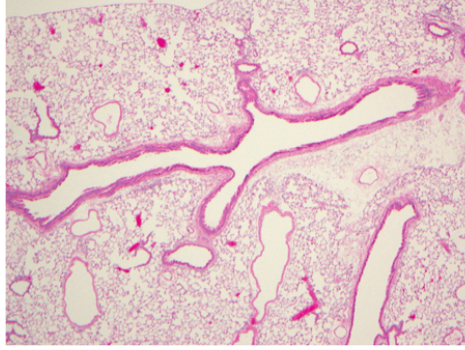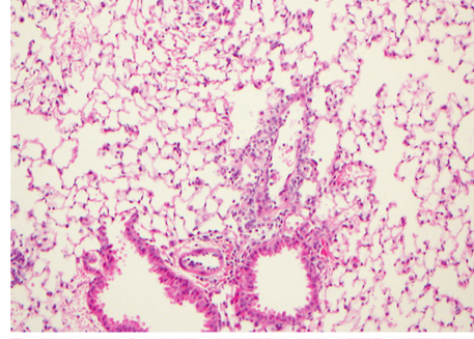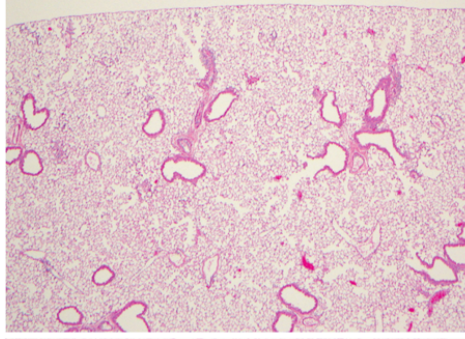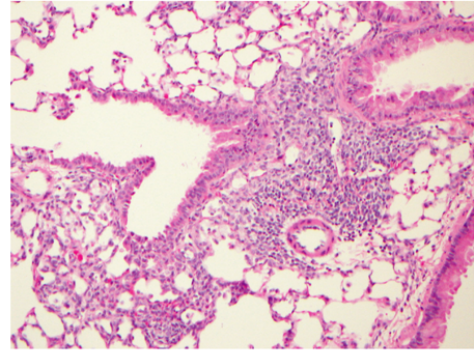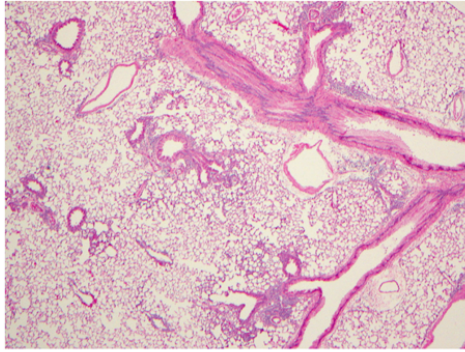
|  | Brainstem | Meninges |
|---|---|---|
| **4 dpi** | | |
| **6 dpi** | | |
| **8 dpi** | | |
| **10 dpi** | | |
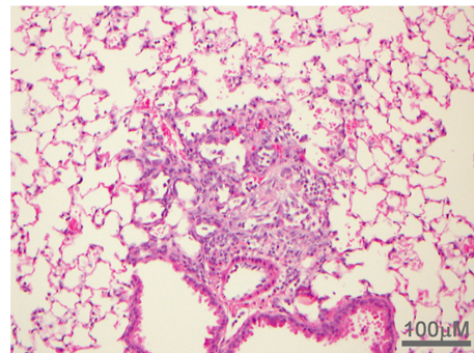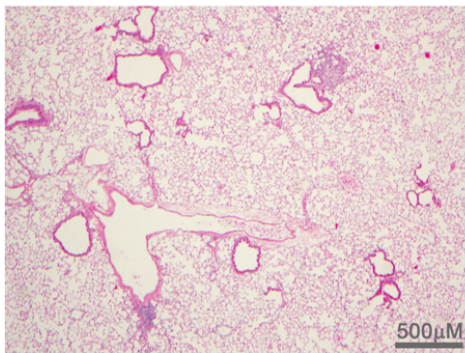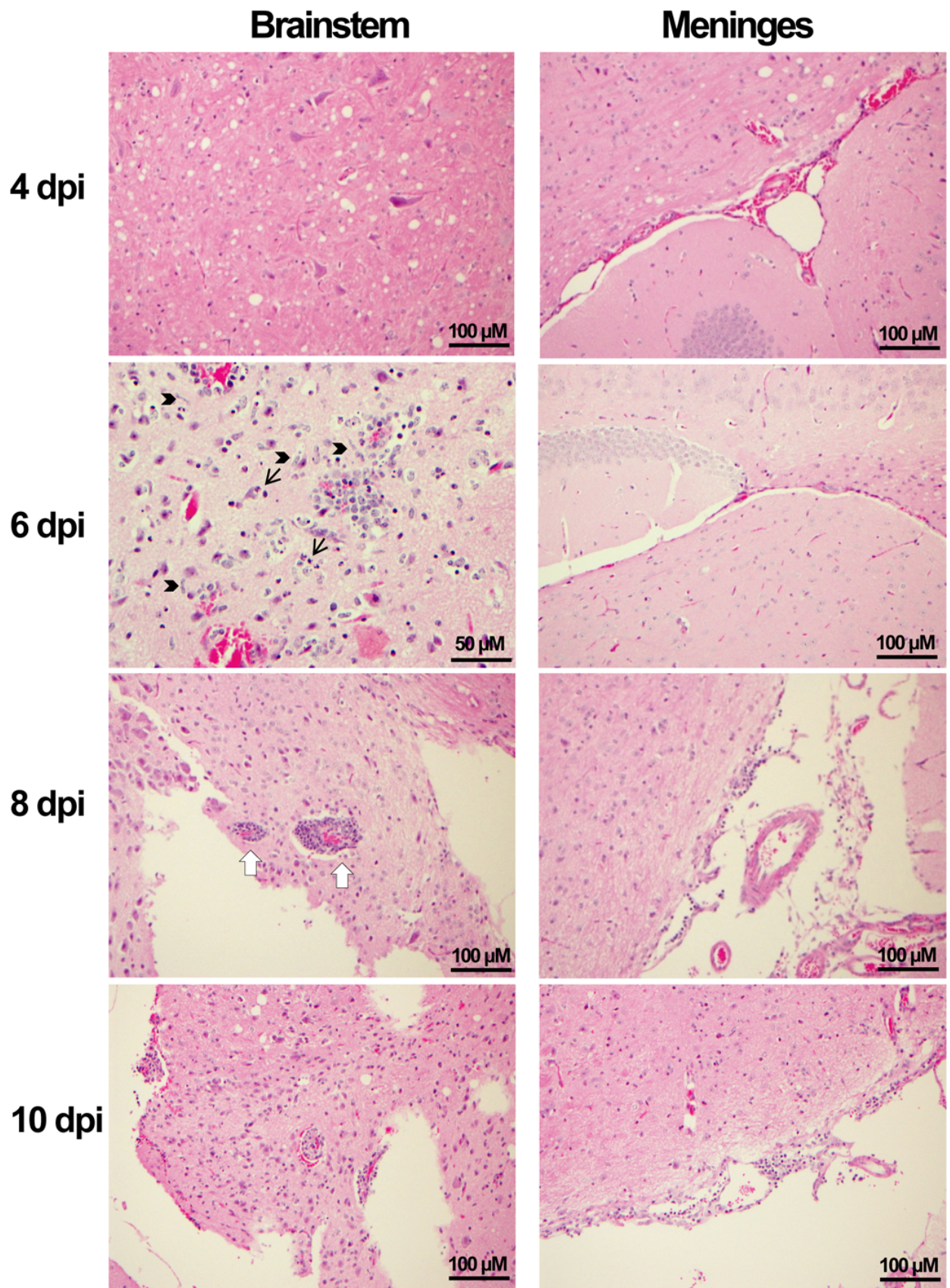


↙: apoptotic body   ➤: activated microglia   ⇧: perivascular cuffing
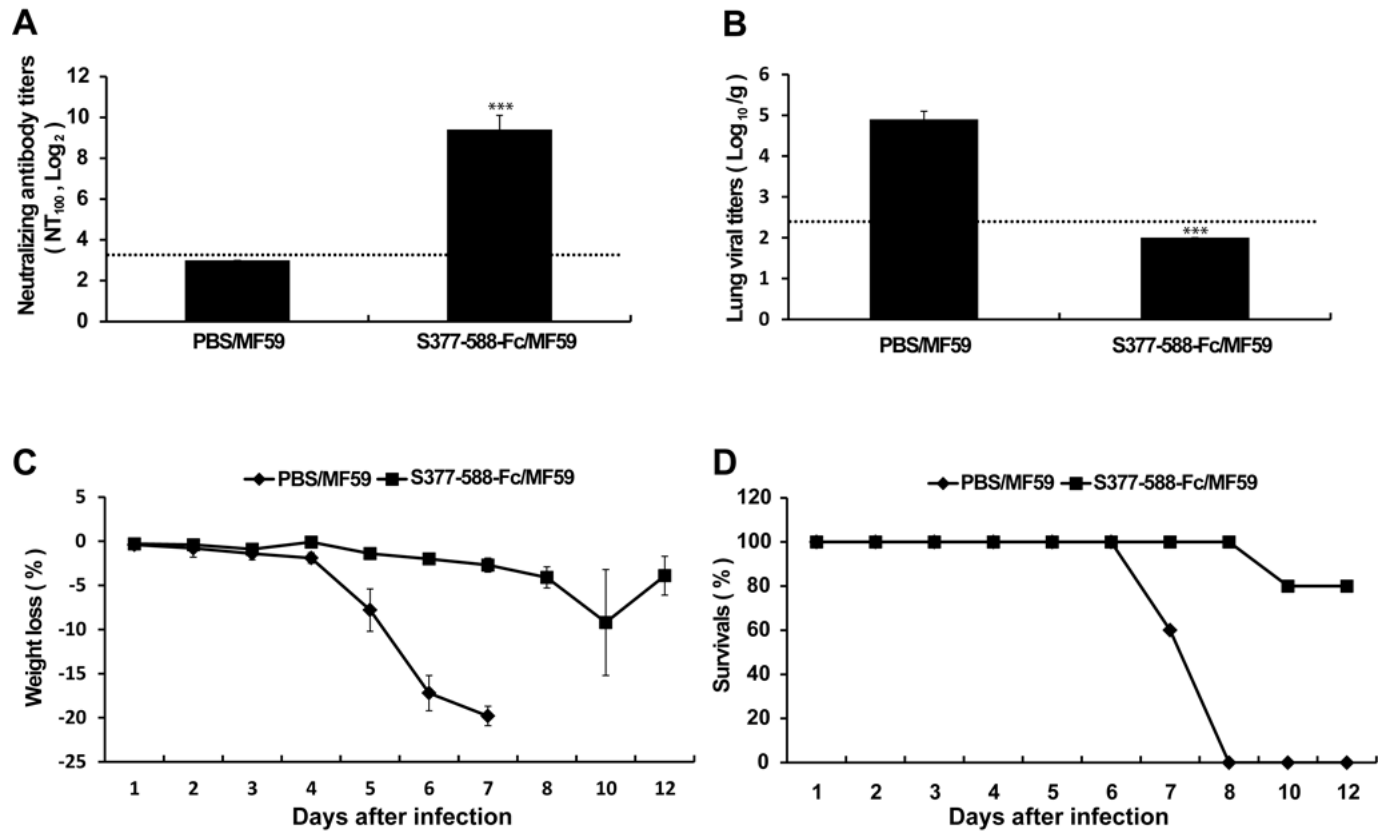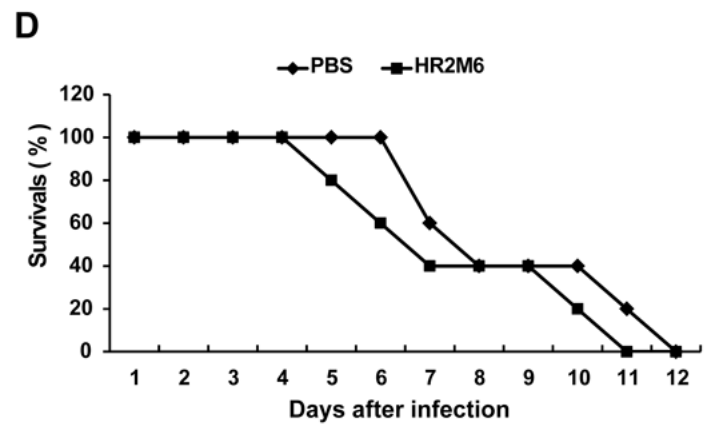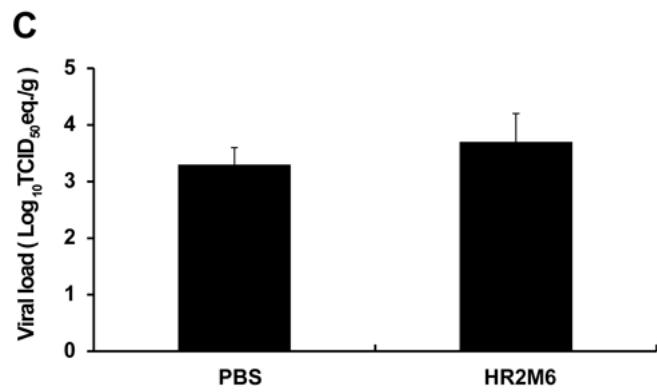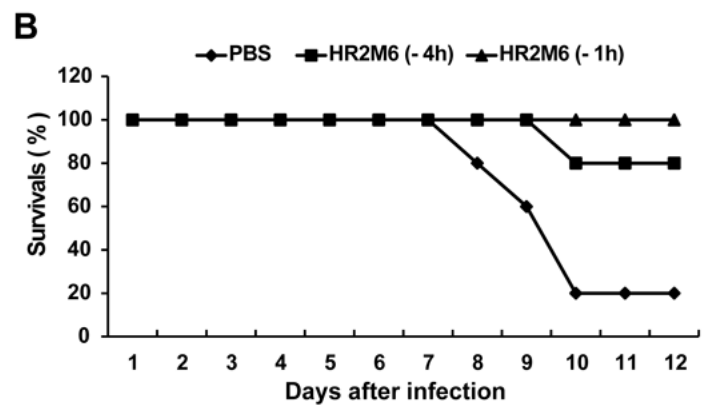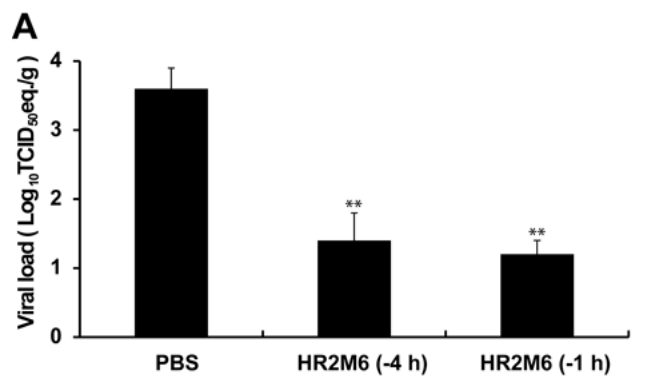
**Table 1.** Determining the 50% lethal dose (LD$_{50}$) and infectious dose (ID$_{50}$) of MERS-CoV in hCD26/DPP4 transgenic mice

| Experiment | Challenge Dose (TCID$_{50}$/mouse) | No. Deaths/No. Challenged (%) | Day of death post challenge | No. infected/No. tested (%)[a] |
|---|---|---|---|---|
| 1 | $10^6$ | 8/8 (100) | 4-6 | NA[b] |
| | $10^5$ | 4/4 (100) | 5-7 | NA |
| | $10^4$ | 4/4 (100) | 5-8 | NA |
| | $10^3$ | 4/4 (100) | 6-10 | NA |
| | $10^2$ | 8/8 (100) | 6-12 | NA |
| | $10^1$ | 5/8 (62.5) | 8-13 | ND[c] |
| 2 | 10 | 2/4 (50) | 9,10 | 2/2 (100) |
| | 5 | 1/4 (25) | 9 | 3/3 (100) |
| | 2.5 | 0/4 (0) | NA[a] | 3/4 (75) |
| | 1.25 | 1/4 (25) | 10 | 3/3 (100) |

a. Infection determined by serum antibody response in neutralization a/o ELISA tests.

b. Not applicable (NA)

c. Not determined (ND)

NOTE: Estimated LD$_{50}$ and ID$_{50}$ are 10 and < 1 TCID$_{50}$, respectively.

**Table 2.** Serum antibody titers to MERS-CoV in survivals of initial challenge and their response to re-challenge

| Initial challenge dose (TCID$_{50}$) | Number of survivors | Serum antibody responses[a] | | |
|---|---|---|---|---|
| | | Neutralizing antibody[b] | ELISA IgG antibody[c] | Death or wt loss on rechallenge[d] |
| 10 | 2 | < 10, 10 | 800,800 | 0/2 |
| 5 | 3 | 10, < 10, 20 | 800,400,800 | 0/3 |
| 2.5 | 4 | 20, 20, < 10, 20 | 400,400,<100, 400 | 0/4 |
| 1.25 | 3 | < 10, 10, < 10 | 400,400,400 | 0/3 |

a: Antibody responses were determined at day 21 p.i.

b: The highest dilution of sera that completely inhibited CPE formation in 100% of infected Vero E6 cultures (NT$_{100}$)

c: The highest dilution of sera with MERS-CoV S1-specific antibody with a mean optical density (OD) ≥ 2 standard deviation (SD) greater than the mean for naïve mice

d: Re-challenged with 100 LD$_{50}$ ($10^{3}$ TCID$_{50}$) of MERS-CoV at day 35 after the initial infection. Two out of two simultaneously challenged naive Tg$^{+}$ mice exhibited severe weight loss ( > 20%) and death occurred within 10 days p.i.